Fission of Polyanionic Metal Clusters

S. König,* A. Jankowski, G. Marx, L. Schweikhard, and M. Wolfram
Institute of Physics, Ernst-Moritz-Arndt University, 17489 Greifswald, Germany

(Received 29 September 2017; published 16 April 2018)

Size-selected dianionic lead clusters Pb_n^{2-}, $n = 34$–56, are stored in a Penning trap and studied with respect to their decay products upon photoexcitation. Contrary to the decay of other dianionic metal clusters, these lead clusters show a variety of decay channels. The mass spectra of the fragments are compared to the corresponding spectra of the monoanionic precursors. This comparison leads to the conclusion that, in the cluster size region below about $n = 48$, the fission reaction $Pb_n^{2-} \rightarrow Pb_{n-10}^- + Pb_{10}^-$ is the major decay process. Its disappearance at larger cluster sizes may be an indication of a nonmetal to metal transition. Recently, the pair of Pb_{10}^- and Pb_{n-10}^- were observed as pronounced fragments in electron-attachment studies [S. König *et al.*, Int. J. Mass Spectrom. **421**, 129 (2017)]. The present findings suggest that this combination is the fingerprint of the decay of doubly charged lead clusters. With this assumption, the dianion clusters have been traced down to Pb_{21}^{2-}, whereas the smallest size for the direct observation was as high as $n = 28$.

DOI: 10.1103/PhysRevLett.120.163001

Just like nuclides show enhanced stability at their magic numbers [1], i.e., when the protons and neutrons fill nuclear shells, atomic clusters also show shell effects. They can have increased stabilities when either their atoms form closed geometric shells, as, in particular, in the case of van der Waals clusters [2], or more closely related to atomic nuclei—when the valence electrons of metal clusters fill electronic shells [3] in the combined Coulomb potential of the ionic cores, as described, e.g., by the jellium model [4,5]. Because of the different strengths of the spin-orbit coupling, the magic numbers of atomic nuclei and metal clusters are not the same [6]. However, similar features have been pointed out, such as the instability toward fission for heavy nuclei and for highly charged metal clusters [7–9]: when their charge is high, nuclei undergo emission of alpha particles or more symmetric fission reactions. Analog behavior has been observed already, more than two decades ago, for multiply charged cationic metal clusters and discussed in detail [10–13]. Both the nuclear and cluster fission can be described in the liquid-drop model. And, indeed, already in the 19th century Lord Rayleigh characterized the stability of charged liquid droplets against breakup due to the charge limit [14,15].

Much more recently, methods have been developed to produce not only highly charged cationic but also anionic metal clusters [16–18]. As in the case of the cations, their stability is limited to larger clusters. However, they have an additional decay pathway, namely, the emission of their excess electrons [19,20]. Up to the present study, polyanionic metal clusters have been observed to either evaporate neutral atoms or to emit electrons, possibly even two electrons simultaneously [21], but, to our knowledge, never an anionic atom or bigger fragment.

In this Letter, we report the first observation of the decay of doubly negatively charged metal clusters into two singly charged product clusters, i.e., fission of dianionic metal clusters. This constitutes a new decay mode. The evidence is based on the comparison of the product pattern from photodissociation of size-selected dianionic clusters with those of the corresponding monoanionic clusters [22]. The conclusion is in line with a previous suggestion of lead-cluster fission in context of the electron-bath application for the production of the polyanionic clusters [23]. In addition, the fission fingerprint allows us to infer in retrospect that small dianionic lead clusters have been produced previously [23], although they could not be observed directly in the corresponding mass spectra.

The experiments have been performed with the ClusterTrap setup [24], which has pioneered the production of polyanionic metal clusters [16,17] and has been further developed over the years [25]. In short, for the present experiment, a laser ablation cluster source [26,27] produces (singly) negatively charged lead clusters. They are guided by ion-optical elements to a linear radio frequency quadrupole trap, a so-called Paul trap. Several cluster bunches are accumulated before they are transferred to a 12-T Penning trap. There, the mixture of clusters of different sizes is exposed to mass-selective excitations of the ion trajectories such that only the clusters of interest remain stored in the trap. Several other experimental steps may follow, as described below.

At the end of a measurement cycle, the Penning trap is emptied by axial ion ejection followed by time-of-flight

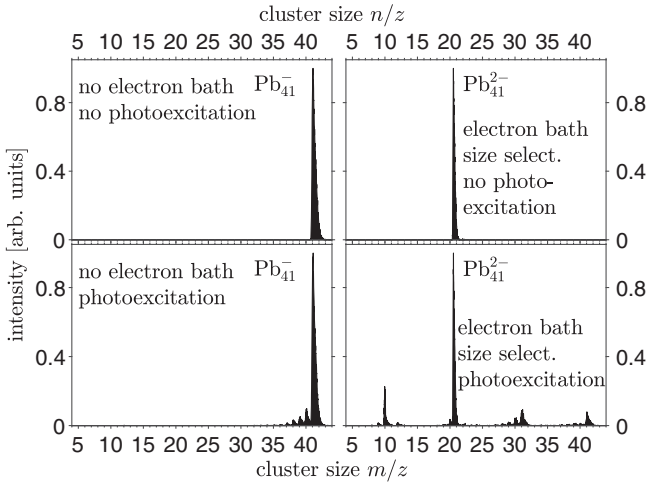

FIG. 1. Abundance spectra of Pb_{41}^- and Pb_{41}^{2-} after size selection of monoanions Pb_{41}^- (top left) and additional photoexcitation (bottom left), after electron bath of Pb_{41}^- followed by size selection of the dianions Pb_{41}^{2-} (top right) and additional photoexcitation (bottom right). (Data of left column taken from the studies reported in [23].)

mass-over-charge (M/Q) analysis. Figure 1 (top left) shows an abundance spectrum, i.e., the ion-signal intensity as a function of ion flight time (from the trap to an ion detector consisting of a conversion electrode and microchannel plates) converted to cluster size over charge state n/z, for the example of Pb_{41}^-.

In a next step, the electron-bath technique [16] can be applied to attach further electrons to the monoanions. This results in the appearance of polyanionic clusters, in the present case, the dianionic lead clusters. In general, additional electrons will only be attached to a fraction of the clusters. In order to perform the following measurements with cluster ions of a defined size and charge state, this is followed by another M/Q, i.e., n/z, selection step. Figure 1 (top right) shows an abundance spectrum from this stage: again, clusters of size $n = 41$ are observed, but now the doubly charged, i.e., at $n/z = 20.5$. (Note that, as the product cluster sizes will be denoted by m, the x axis is labeled "m/z," although the spectra include the signal of the remaining precursor clusters.)

The size and charge-state selected clusters are subjected to a laser pulse (wavelength of 532 nm, pulse duration of about 4 ns, pulse energy of about 3 mJ, and beam diameter of about 9 mm); see Fig. 1, bottom left and right. In general, the photoexcitation leads to some kind of decay reaction. Noble metal clusters, e.g., decay by evaporation of neutral atoms or dimers [28–30] or by electron emission [21,31]. As these processes may occur delayed [32–36], a waiting time (100 ms) is applied between the laser excitation and product analysis. Most of the previous steps, such as the n/z selection, take about an order of magnitude more time. Thus, typical measurement cycles are several seconds long. The number of cluster ions detected per cycle is between a few up to about 200. The cycles are repeated 80–450 times to increase the statistical significance of the data.

In the following, we will first focus on the particular case of Pb_{44}^{2-}. This is the smallest lead cluster where Pb_{n-10}^{2-}, i.e., Pb_{34}^{2-}, was available in sufficient amounts for photoexcitation studies. The importance of this relation will be obvious from the discussion further below. Figure 2 shows the abundance spectrum after photoexcitation of size-selected Pb_{44}^{2-}. In addition to the smaller dianions Pb_{43}^{2-}, Pb_{42}^{2-}, and Pb_{41}^{2-}, due to sequential monomer evaporation, there are three distinct regions of decay products, at Pb_{44}^- and below, Pb_{34}^- and below, and Pb_{10}^- with a small Pb_9^- signal nearby. (The charge states of the ions in the four regions are inferred from the presence or nonpresence of signals at half-integer m/z values.) Obviously, Pb_{44}^- can only be produced by electron emission,

$$Pb_{44}^{2-} + h\nu \rightarrow Pb_{44}^- + e^-. \tag{1}$$

In general, the monoanionic product can still have some excitation energy and thus be able to decay further. The decay patterns of the monoanions are already known from a recent photoexcitation study [22]. Figure 3 (top) shows the result for Pb_{44}^-: sequential monomer evaporation:

$$\begin{aligned} Pb_{44}^{2-} + h\nu \rightarrow\ & Pb_{44}^{-\,*} + e^- \\ & \hookrightarrow Pb_{43}^{-\,*} + Pb \\ & \quad \hookrightarrow Pb_{42}^{-\,*} + Pb \\ & \quad\quad \hookrightarrow \ldots \end{aligned} \tag{2}$$

This explains the present observation at Pb_{44}^-, as well as for the product ions down to about Pb_{35}^-.

Without further information, the Pb_{34}^- and Pb_{10}^- products could be due to several decay pathways:

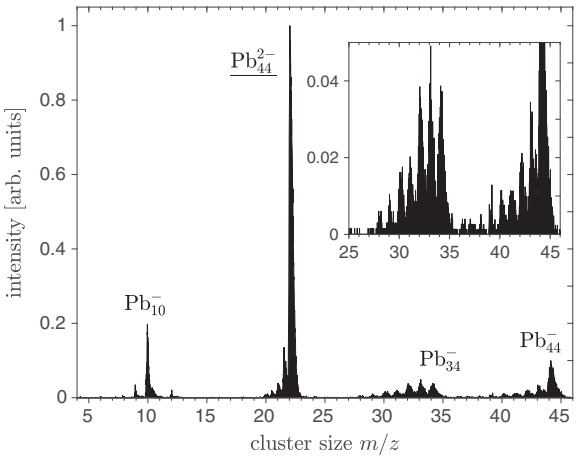

FIG. 2. Abundance spectrum of size selected and photoexcited Pb_{44}^{2-} clusters (label of the precursor underlined, as also in the following spectra).

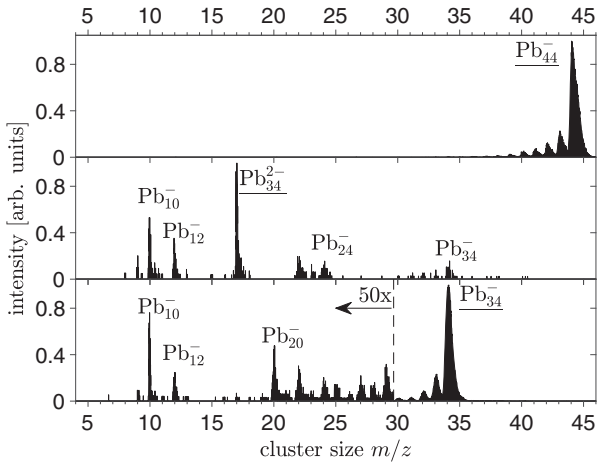

FIG. 3. Abundance spectrum of Pb_{44}^- (top), Pb_{34}^- (bottom), and Pb_{34}^{2-} (middle) after photoexcitation. (Data for top and bottom taken from Ref. [22].)

(i) electron emission followed by the breaking off of a neutral decamer Pb_{10}, resulting in the Pb_{34}^- signal

$$\begin{aligned} Pb_{44}^{2-} + h\nu \rightarrow\ & Pb_{44}^{-\,*} + e^- \\ & \hookrightarrow Pb_{34}^- + Pb_{10} \end{aligned} \tag{3}$$

(ii) similar to reaction (3) with the electron now staying attached to the decamer

$$\begin{aligned} Pb_{44}^{2-} + h\nu \rightarrow\ & Pb_{44}^{-\,*} + e^- \\ & \hookrightarrow Pb_{34} + Pb_{10}^- \end{aligned} \tag{4}$$

(iii) again, similar to reaction (3), but now with a further sequential decay to produce Pb_{10}^-

$$\begin{aligned} Pb_{44}^{2-} + h\nu \rightarrow\ & Pb_{44}^{-\,*} + e^- \\ & \hookrightarrow Pb_{34}^{-\,*} + Pb_{10} \\ & \quad \hookrightarrow Pb_{10}^- + Pb_{24} \end{aligned} \tag{5}$$

(iv) again, similar to reaction (3), but in reverse order, i.e., first breaking off of a neutral Pb_{10} followed by electron emission from the remaining doubly charged Pb_{34}^{2-}

$$\begin{aligned} Pb_{44}^{2-} + h\nu \rightarrow\ & Pb_{34}^{2-\,*} + Pb_{10} \\ & \hookrightarrow Pb_{34}^- + e^- \end{aligned} \tag{6}$$

Note that in all these processes, each one accounts for only one of the products, either Pb_{34}^- or Pb_{10}^-. Thus, it takes at least two of them to explain the observation of both in the decay spectrum. In contrast, and last but not least, the simple fission process

$$Pb_{44}^{2-} + h\nu \rightarrow Pb_{34}^- + Pb_{10}^- \tag{7}$$

leads to a simultaneous production of both product cluster ions.

Next, the decay pathways (3)–(6) are further examined by inspecting the decays of the intermediate fragments, Pb_{44}^-, Pb_{34}^-, and Pb_{34}^{2-}. The decay of Pb_{44}^- has already been discussed above. Only sequential monomer evaporation was found, but no sign of a decay to Pb_{34}^- or Pb_{10}^-. This excludes reactions (3) and (4) and also (5). The latter is, additionally, not expected as the analog final step with the excess electron ending up on Pb_{24} instead of Pb_{10} is not observed.

In order to investigate the possibility of reaction (6), one can have a look at the decay of size-selected and photoexcited dianionic Pb_{34}^{2-} (see Fig. 3, middle): there are several fragments observed, namely, Pb_{10}^-, Pb_{12}^-, Pb_{22}^-, and Pb_{24}^-, and also a monomer evaporation chain starting with Pb_{34}^-. In Fig. 2, however, no fragments of Pb_{24}^- can be found and the abundance ratio between Pb_{10}^- and Pb_{12}^- is quite different. Thus, the product fingerprint of Pb_{34}^{2-} is missing. Additionally, there is no signal of Pb_{34}^{2-} in Fig. 2 (which would appear at $m/z = 17$). Furthermore, Fig. 3 (bottom) shows the photoexcitation spectrum of Pb_{34}^-, where each cluster size from Pb_{34}^- down to Pb_{20}^- is observed, in contrast to the decay pattern of Pb_{44}^{2-}. Therefore, reaction (6) can be ruled out as a pathway to Pb_{34}^-.

In conclusion, the only remaining explanation for the appearance of the fragments Pb_{10}^- and Pb_{34}^- in Fig. 2 (and Pb_{33}^-, Pb_{32}^-, etc., which result from sequential monomer evaporation from Pb_{34}^-) is reaction (7), the fission of Pb_{44}^{2-} into Pb_{34}^- and Pb_{10}^-. A similar behavior was reported for doubly positively charged noble metal clusters Cu_n^{2+}, Ag_n^{2+}, and Au_n^{2+}. There, fission into clusters with closed electronic shells Cu_3^+ [37], Ag_3^+, Ag_9^+ [38], and Au_3^+, Au_9^+ [7] was observed.

The photodissociation measurements on dianionic lead clusters have been performed with smaller precursors down to $n = 34$, the lowest cluster size where sufficiently many dianions could be produced for further investigations. At the upper cluster size end, the investigations were extended up to $n = 56$.

The results are summarized in Fig. 4. Each horizontal line represents the photofragmentation mass spectrum of a precursor cluster size n, indicated on the y axis. The signal of the precursor cluster Pb_n^{2-} appears at $m/z = n/2$. Another pronounced line lies at $m = n$; these signals are due to the clusters Pb_n^-, i.e., clusters that emitted one of the two excess electrons. Further strong signals occur at $m/z = n - 10$ and at $m/z = 10$, 12, and also at 20. The clusters Pb_{n-10}^- and Pb_{10}^- from precursor clusters Pb_{34}^{2-} up to Pb_{48}^{2-} can be explained by a fission process of the dianion, as described above for the case of Pb_{44}^{2-} into the singly charged clusters Pb_{n-10}^- and Pb_{10}^-, which is known to have a particularly high stability [22,23,31,39].

Interestingly, the fission processes end at precursor cluster size $n \approx 48$. This is in agreement with the results

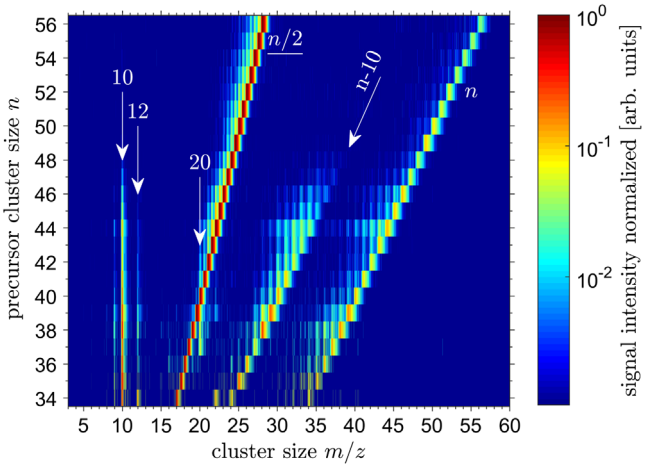

FIG. 4. Intensity plot of the abundance of size-selected and photoexcited lead-cluster dianions $n/2$. The color represents the signal height with logarithm scaling. Each horizontal line is normalized to the highest signal. The most prominent line at $m/z = n/2$ is due to the remaining precursor clusters Pb_n^{2-} (label $n/2$, underlined).

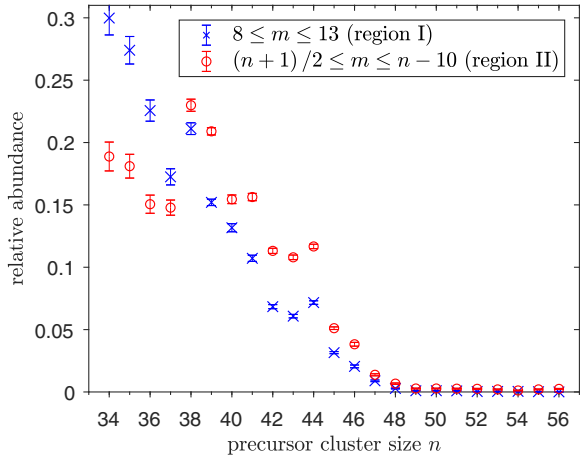

FIG. 5. Relative abundance of the sum of $Pb^-_{8,\ldots,13}$ (blue) and $Pb^-_{(n+1)/2,\ldots,n-10}$ (red) for each precursor Pb_n^{2-}.

of electron-beam interaction measurements [23]. Possibly, there is a structural change around this cluster size. In contrast to the electron-interaction measurements [23], no pronounced signal line at cluster size $m = n - 12$ can be found except for the precursor cluster size $n = 34$. Possibly, the energy needed for such a fission process is higher than the energy provided by the present photoexcitation. From cluster size $n = 37$ up to $n = 44$, a pronounced signal can be found for the cluster $m = 20$, in agreement with previous findings [22,23]. The highest signal for $m = 20$ (except where it cannot be distinguished from doubly charged products) is found for the fragmentation of Pb_{37}^{2-}, presumably because the cluster fissions into cluster size Pb_{27}^- and further evaporates a neutral Pb_7 cluster,

$$\begin{aligned} Pb_{37}^{2-} + h\nu \rightarrow\ & Pb_{27}^{-*} + Pb_{10}^- \\ & \hookrightarrow Pb_{20}^- + Pb_7, \end{aligned} \tag{8}$$

a major decay process in earlier measurements [22,23].

If the dianions decay mainly by fission into two charged clusters $Pb^-_{n-10,n-12}$ and $Pb^-_{10,12}$, the abundance of both charged fragments should be similar. In Fig. 5, the relative abundance of both fission constituents $Pb^-_{n-10,n-12}$ and $Pb^-_{10,12}$ are given, with the integration borders shown in Fig. 6 for the example of Pb_{38}^{2-}. Region I includes the clusters $Pb^-_{8,\ldots,13}$ and region II $Pb^-_{(n+1)/2,\ldots,n-10}$. The relative abundances (Fig. 5) show the same trend with similar values. The small differences could be caused by further evaporation of neutrals from Pb^-_{n-10}, including Pb^-_{20}, which cannot be distinguished from the precursor in some cases, or by different transfer and detection efficiencies as a function of cluster size.

The relative abundance of both fission products is decreasing with increasing cluster size. In contrast, up to the largest precursor clusters, monomer evaporation and electron detachment is observed as predicted by the liquid-drop model [40]. This may indicate a nonmetal to metal transition in the cluster size region of $n \approx 48$, in agreement with ion mobility experiments, where no transition was found up to $n = 32$ [41]. In contrast, theoretical considerations [42] and photoelectron spectroscopy measurements [43] suggested $n \approx 20$ as the transition region.

Already in the lead-cluster investigations with the aim of electron attachment for di- and trianion production [23], hints were found for fission processes of dianionic clusters: as in the present dianion photoexcitation measurements, from precursor cluster size $n \approx 48$ downward, Pb_m^- clusters

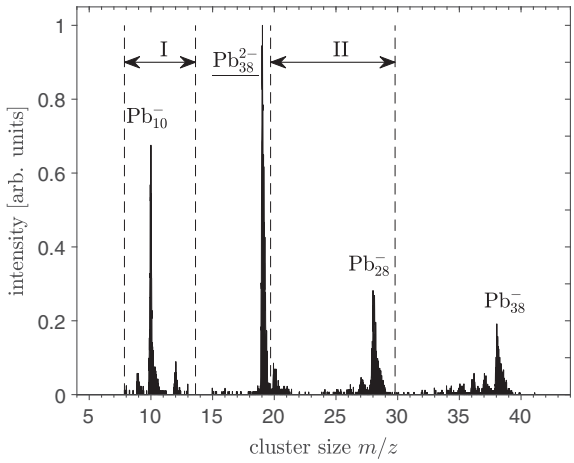

FIG. 6. Abundance spectrum of Pb_{38}^{2-} after photoexcitation. The dashed lines and double arrows I and II indicate integration borders for fragments $Pb^-_{8,\ldots,13}$ and $Pb_{(n+1)/2,\ldots,n-10}$ (for details, see text).

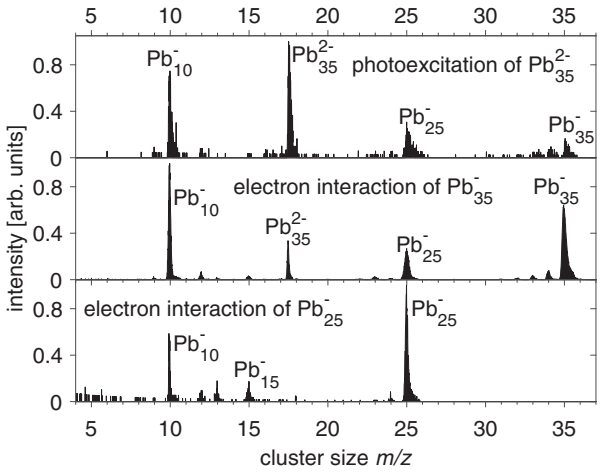

FIG. 7. Abundance spectra after photoexcitation of Pb_{35}^{2-} (top), after electron interaction of Pb_{35}^{-} [23] (middle), and after electron interaction of Pb_{25}^{-} [23] (bottom).

were observed with $m = n - 10$. As an example, the abundance spectra after photoexcitation of Pb_{35}^{2-} and after electron interaction of Pb_{35}^{-} are given in Fig. 7. Both spectra show the fragments Pb_{10}^{-} and Pb_{25}^{-} beside the fragments and precursor clusters Pb_{35}^{-} and Pb_{35}^{2-} and their monomer evaporation chain.

While Pb_{34}^{2-} was the smallest precursor cluster accessible for the present photoexcitation studies, the previous electron-attachment investigations could be continued down to smaller clusters [23]. By use of the fragment $m = n - 10$ as an indicator of fission process, this process is accessible even without the direct observation of dianionic precursors, as in the case of Pb_{25}^{2-} (Fig. 7, bottom). The smallest fission precursor (indirectly) observed in this way is the dianion Pb_{21}^{2-}, as the line of fragments Pb_{n-10}^{-} can be trailed down (at least) to Pb_{11}^{-} (Fig. 8 in [23]). In contrast, the smallest dianionic lead cluster observed directly until now has a size of $n = 28$ [23]. Thus, a new tool has been found that extends the observation range of the dianion precursors significantly.

This work was supported by the Collaborative Research Center of the DFG (SFB 652-TP A03).

*Stephan.Koenig@physik.uni-greifswald.de

[1] M. G. Mayer and J. H. D. Jensen, *Elementary Theory of Nuclear Shell Structure* (Wiley, New York, 1964).
[2] O. Echt, K. Sattler, and E. Recknagel, Magic Numbers for Sphere Packings: Experimental Verification in Free Xenon Clusters, Phys. Rev. Lett. **47**, 1121 (1981).
[3] W. D. Knight, K. Clemenger, W. A. de Heer, W. A. Saunders, M. Y. Chou, and M. L. Cohen, Electronic Shell Structure and Abundances of Sodium Clusters, Phys. Rev. Lett. **52**, 2141 (1984).
[4] W. Ekardt, Work function of small metal particles: Self-consistent spherical jellium-background model, Phys. Rev. B **29**, 1558 (1984).
[5] J. P. Perdew, Energetics of charged metallic particles: From atom to bulk solid, Phys. Rev. B **37**, 6175 (1988).
[6] S. Bjørnholm, Similarities and differences between atomic nuclei and clusters, AIP Conf. Proc. **416**, 7 (1997).
[7] W. A. Saunders, Metal-cluster fission and the liquid-drop model, Phys. Rev. A **46**, 7028 (1992).
[8] S. Bjørnholm, Fission of nuclei and metal clusters, Surf. Rev. Lett. **03**, 623 (1996).
[9] P.-G. Reinhard and E. Suraud, *Introduction to Cluster Dynamics* (Wiley, Weinheim, 2003).
[10] U. Näher, S. Bjørnholm, S. Frauendorf, F. Garcias, and C. Guet, Fission of metal clusters, Phys. Rep. **285**, 245 (1997).
[11] A. Lyalin, O. I. Obolensky, A. V. Solov'yov, and W. Greiner, Fission of metal clusters, Int. J. Mod. Phys. E **15**, 153 (2006).
[12] P. M. Dinh, P. G. Reinhard, and E. Suraud, Time-resolved fission of metal clusters and nuclei, Int. J. Mod. Phys. E **17**, 120 (2008).
[13] D. N. Poenaru, R. A. Gherghescu, and W. Greiner, Fissility of nuclear and atomic cluster systems, Romanian reports in Physics **63**, 1133 (2011).
[14] Lord Rayleigh, On the equilibrium of liquid conducting masses charged with electricity, Philos. Mag. **14**, 184 (1882).
[15] D. Duft, T. Achtzehn, R. Müller, B. A. Huber, and T. Leisner, Coulomb fission: Rayleigh jets from levitated microdroplets, Nature (London) **421**, 128 (2003).
[16] A. Herlert, S. Krückeberg, L. Schweikhard, M. Vogel, and C. Walther, First observation of doubly charged negative gold cluster ions, Phys. Scr. **T80**, 200 (1999).
[17] C. Yannouleas, U. Landman, A. Herlert, and L. Schweikhard, Multiply Charged Metal Cluster Anions, Phys. Rev. Lett. **86**, 2996 (2001).
[18] C. Stoermer, J. Friedrich, and M. M. Kappes, Observation of multiply charged cluster anions upon pulsed UV laser ablation of metal surfaces under high vacuum, Int. J. Mass Spectrom. **206**, 63 (2001).
[19] M. K. Scheller, R. N. Compton, and L. S. Cederbaum, Gas-phase multiply charged anions, Science **270**, 1160 (1995).
[20] X.-B. Wang and L.-S. Wang, Experimental Search for the Smallest Stable Multiply Charged Anions in the Gas Phase, Phys. Rev. Lett. **83**, 3402 (1999).
[21] A. Herlert and L. Schweikhard, Two-electron emission after photoexcitation of metal-cluster dianions, New J. Phys. **14**, 055015 (2012).
[22] S. König, F. Martinez, L. Schweikhard, and M. Wolfram, Photodecay pathways of stored, size-selected lead clusters Pb_n^+, $n = 6 - 41$ and Pb_n^- $n = 9 - 56$, J. Phys. Chem. C **121**, 10858 (2017).
[23] S. König, S. Bandelow, L. Schweikhard, and M. Wolfram, Interaction of anionic lead clusters Pb_n^-, $n = 10$, 12-102 with electrons–Polyanion production and cluster decay, Int. J. Mass Spectrom. **421**, 129 (2017).
[24] L. Schweikhard, S. Krückeberg, K. Lützenkirchen, and C. Walther, The Mainz cluster trap, Eur. Phys. J. D **9**, 15 (1999).

[25] F. Martinez, S. Bandelow, C. Breitenfeldt, G. Marx, L. Schweikhard, A. Vass, and F. Wienholtz, Upgrades at ClusterTrap and latest results, Int. J. Mass Spectrom. **365–366**, 266 (2014).
[26] T. G. Dietz, M. A. Duncan, D. E. Powers, and R. E. Smalley, Laser production of supersonic metal cluster beams, J. Chem. Phys. **74**, 6511 (1981).
[27] H. Weidele, U. Frenzel, T. Leisner, and D. Kreisle, Production of "cold/hot" metal cluster ions: A modified laser vaporization source, Z. Phys. D **20**, 411 (1991).
[28] V. A. Spasov, T. H. Lee, J. P. Maberry, and K. M. Ervin, Measurement of the dissociation energies of anionic silver clusters (Ag_n^-, n=2–11) by collision-induced dissociation, J. Chem. Phys. **110**, 5208 (1999).
[29] O. Ingólfsson, U. Busolt, and K.-i. Sugawara, Energy-resolved collision-induced dissociation of Cu_n^+ (n=2–9): Stability and fragmentation pathways, J. Chem. Phys. **112**, 4613 (2000).
[30] M. Vogel, A. Herlert, and L. Schweikhard, Photodissociation of small group-11 metal cluster ions: Fragmentation pathways and photoabsorption cross sections, J. Am. Soc. Mass Spectrom. **14**, 614 (2003).
[31] G. Ganteför, M. Gausa, K. H. Meiwes-Broer, and H. O. Lutz, Photoemission from tin and lead cluster anions, Z. Phys. D **12**, 405 (1989).
[32] P. Wurz and K. R. Lykke, Delayed electron emission from photoexcited C_{60}, J. Chem. Phys. **95**, 7008 (1991).
[33] Y. Shi, V. A. Spasov, and K. M. Ervin, Competitive fragmentation and electron loss kinetics of photoactivated silver cluster anions: Dissociation energies of Ag_n^- (n=7–11), J. Chem. Phys. **111**, 938 (1999).
[34] M. Vogel, K. Hansen, A. Herlert, and L. Schweikhard, Model-Free Determination of Dissociation Energies of Polyatomic Systems, Phys. Rev. Lett. **87**, 013401 (2001).
[35] M. Vogel, K. Hansen, A. Herlert, and L. Schweikhard, Decay pathways of small gold clusters, Eur. Phys. J. D **16**, 73 (2001).
[36] M. Wolfram, S. König, S. Bandelow, P. Fischer, A. Jankowski, G. Marx, and L. Schweikhard, Disentangling the photodissociation pathways of small lead clusters by time-resolved monitoring of their delayed decays: The case of Pb_{31}^+, J. Phys. B **51**, 044005 (2018).
[37] S. Krückeberg, L. Schweikhard, J. Ziegler, G. Dietrich, K. Lützenkirchen, and C. Walther, Decay pathways and dissociation energies of copper clusters, Cu_n^+ ($2 \leq n \leq 25$), Cu_n^{2+} ($15 \leq n \leq 25$), J. Chem. Phys. **114**, 2955 (2001).
[38] I. Katakuse, H. Ito, and T. Ichihara, Fission-like dissociation of doubly charged silver clusters, Int. J. Mass Spectrom. Ion Process. **97**, 47 (1990).
[39] C. Lüder and K. Meiwes-Broer, Electron detachment energies of Pb_N^- ($N = 24 - 204$) determined in a simple magnetic bottle photoelectron spectrometer, Chem. Phys. Lett. **294**, 391 (1998).
[40] C. Yannouleas and U. Landman, Multiply charged anionic metal clusters, Chem. Phys. Lett. **210**, 437 (1993).
[41] A. A. Shvartsburg and M. F. Jarrold, Transition from covalent to metallic behavior in group-14 clusters, Chem. Phys. Lett. **317**, 615 (2000).
[42] B. Wang, J. Zhao, X. Chen, D. Shi, and G. Wang, Atomic structures and covalent-to-metallic transition of lead clusters Pb_n ($n = 2 - 22$), Phys. Rev. A **71**, 033201 (2005).
[43] V. Senz *et al.*, Core-Hole Screening as a Probe for a Metal-to-Nonmetal Transition in Lead Clusters, Phys. Rev. Lett. **102**, 138303 (2009).